Relationship between denitrification performance and microbial community structure in a PHBV-supported denitrification reactor

Shusong Zhang[a], Yueting Fan[b], Nan Zhang[c], Xuming Wang[d],*

[a]*College of Ocean and Bioengineering, Yancheng Teachers University, Yancheng 224007, China, email: zhangshusong1106@163.com*
[b]*Environmental Protection Key Laboratory of Source Water Protection, Chinese Research Academy of Environmental Sciences, Beijing 100012, China, email: 361456933@qq.com*
[c]*Jiangsu Nuclear Power Corporation, Lianyungang 222002, China, email: 123076718@qq.com*
[d]*Beijing Agro-Biotechnology Research Center, Beijing Academy of Agriculture and Forestry Sciences, Beijing 100097, China, email:wangxm413@163.com*

ABSTRACT

Solid-phase denitrification systems using biodegradable polymers are promising for wastewater treatment; however, little is known about the relationship between microbial communities and effluent quality in these systems. In this study, we evaluated the performance of a poly(3-hydroxybutyrate-*co*-3-hydroxyvalerate) (PHBV)-supported denitrification system in the treatment of wastewater with high nitrate concentrations with respect to the microbial community structure and dominant bacteria. An average denitrification rate of 1.11 g/(L d) could be achieved at an influent NO_3^-–N concentration of 80 mg/L and hydraulic retention time (HRT) of 1.5 h. Compared to the HRT, the influent NO_3^-–N concentration had a greater effect on the denitrification efficiency at the same NO_3^-–N loading rate (NLR). Microbial community analysis using Miseq Illumina sequencing showed that the genera *Diaphorobacter* and *Dechloromonas* were predominant. The nitrate removal efficiency was positively correlated with the *Dechloromonas* abundance, and the NLR was negatively correlated with *Diaphorobacter*. Heatmap analysis showed that the denitrification function dominated over all stages, which may explain the good performance of the PHBV-supported denitrification system. These findings clarify the effect of the influent nitrate load on microbial functional abundance and community structure as well as the molecular determinants of solid-phase denitrification efficiency.

Keywords: Solid-phase denitrification; Poly(3-hydroxybutyrate-*co*-3-hydroxyvalerate); Microbial community; Functional analysis

1. Introduction

Biological nitrate removal is widely applied for wastewater treatment owing to its low cost and high efficiency. During the biological denitrification process, organic carbon is used as an electron donor by heterotrophic microorganisms [1]. External organic carbon should be added during the process, especially when treating wastewater with a low C/N ratio, such as groundwater, and during

tertiary nitrogen removal from wastewater treatment plants [2,3]. Insufficient dosing or overdosing of conventional soluble carbon sources, such as methanol, ethanol, sodium acetate, and glucose, can lead to the deterioration of effluent quality. In addition, soluble carbon sources pose safety risks owing to their toxicity and flammability during storage, transportation, and operation [4]. To overcome these issues, insoluble biodegradable polymers have recently been used as carbon sources and biofilm carriers in the biological denitrification of wastewater, known as solid-phase

* Corresponding author.

denitrification (SPD) [5,6]. SPD enables the simple control and supervision of the process [7] and is therefore widely used for nitrate removal.

Within the SPD system, two processes occur: hydrolysis and denitrification. The hydrolysis of the solid carbon source by extracellular enzymes excreted by degrading microorganisms is the first and most important step, followed by the use of the degradation products by denitrifying bacteria [8]. Previous studies have identified various microorganisms such as *Thauera*, *Dechloromonas*, and *Clostridium*, which play roles in degradation and denitrification during the SPD processing of poly(3-hydroxybutyrate-*co*-3-hydroxyvalerate)/poly(lactic acid) (PHBV/PLA) and PHBV biofilms [8,9]. These bacteria can utilize carbohydrates or mono-aromatic compounds and biodegradable polymers completely as carbon and energy sources for denitrification to produce N_2 and volatile fatty acids such as acetate, butyrate, and butanol [10,11]. These bacteria commonly occupy a dominant position in the system to promote biological denitrification. The microbial community structure is greatly affected by external environmental conditions such as temperature and salinity. For example, *Thauera*, *Nitrospira*, *Arenimonas*, and *Dechloromonas* biofilms are rarely found in SPD biofilters; nevertheless, they become dominant in low-temperature environments [12]. However, the relationship between bacterial communities in the SPD system and effluent quality has rarely been reported, despite being significant for controlling the nitrogen removal efficiency in water treatment.

In this study, we used PHBVs as biofilm carriers and carbon sources in an SPD system. The objectives of the study were to (1) evaluate the denitrification performance of the system, (2) characterize microbial diversity under different operational conditions by high-throughput sequencing, and (3) explore the relationship between the microbial community structure and denitrification performance of the system. The microflora structure of the reactor is regulated by changes in water quality parameters, thereby influencing operating efficiency. Our results provide a comprehensive basis for understanding the microbial community structure in the SPD process.

2. Materials and methods

2.1. Materials

Biodegradable PHBV granules were purchased from Ningbo Biologic Material Co., Ltd., (Zhejiang, China). The physical characteristics of the PHBV granules were

as follows: diameter, 3 mm; height, 2–3 mm; surface area 0.015 m^2/g; and density, 1.25 kg/L.

To represent wastewater with a low C/N ratio, synthetic wastewater was prepared by adding $NaNO_3$ and KH_2PO_4 to tap water. The seed for denitrification was activated sludge collected from an anaerobic treatment tank in the municipal wastewater treatment plant. The sludge contained 3,450 mg/L mixed liquid-suspended solids and 2,910 mg/L volatile suspended solids, and the sludge-settling percentage was 30%.

2.2. Experimental setup

This study employed an up-flow fixed-bed reactor filled with PHBV granules (350 g) made from the 50-mm-inner diameter and 600-mm-high cylindrical Plexiglas. The reactor had an effective volume of 0.75 L (Fig. S1). The synthetic wastewater containing activated sludge was pumped into the bottom of the reactor by a peristaltic pump at a flow rate of 2.0 mL/min hydraulic retention time (HRT ≈ 6.5 h) at the domestication stage. The steady-state of the bioreactor was regarded as the point at which fluctuations in the removal of nitrate were ±5% for 5 d. After stable denitrification was obtained, the flow rate and influent nitrate concentration were increased stepwise to evaluate the effect of the nitrate loading rates. The PHBV denitrification system operations are summarized in Table 1. The temperature of the reactor was 25°C ± 1°C, and the pH was maintained at 7.0–7.3. Samples were taken from the effluent to monitor NO_3^-–N, NO_2^-–N, NH_4^+–N, and dissolved organic carbon (DOC).

2.3. Water quality analytical methods

The influent and effluent of the reactor were collected and analyzed daily. Before the analysis, the water samples were filtered through a 0.45 μm membrane. NO_3^-–N, NO_2^-–N, and NH_4^+–N were measured by ultraviolet spectrophotometry, *N*-(1-naphthalene)-diaminoethane spectrophotometry, and Nessler's reagent spectrophotometry, respectively, in accordance with the methods described by Zhang et al. [4]. DOC was measured using a TOC analyzer (Element, Berlin, Germany) through combustion oxidation-non-dispersive infrared absorption.

2.4. Microbial community analysis

Attached biofilm samples were collected by ultrasonic treatment (Shumei, Kunshan, China) from the PHBV

Table 1
Operational parameters for the PHBV reactor

Phase	Time (d)	Hydraulic retention time (h)	NO_3^-–N concentration (mg/L)	NLR (g/(L d))
Acclimatization	0–13	6.5	80	–
1	14–47	6.5	80	0.30
2	48–68	2.5	80	0.77
3	69–89	1.5	80	1.28
4	90–113	1.9	100	1.28

granules of the reactor on days 30, 61, 81, and 105. PowerSoil DNA Isolation Kits (MoBio Laboratories, Carlsbad, CA, USA) were used to extract DNA from the biofilm samples. The DNA quality was visualized on TAE agarose gels. The quantity and yield were checked using a NanoDrop 1000 Spectrophotometer (Thermo Scientific, Waltham, MA, USA) to make sure the DNA concentration was >20 ng/μL. Primers 338F (5′-ACTCCTACGGGAGGCAGCAG-3′) and 806R (5′-GGACTACHVGGGTWTCTAAT-3′) were used to amplify the V4–V5 regions of the bacterial genome. The reaction system and procedures for PCR amplification are detailed in the Supplementary Material (Tables S1 and S2).

The DNA samples were sent to Novogene Biotechnology Co., Ltd., (Beijing, China) for Illumina high-through-put sequencing using the HiSeq 2500 system (Illumina, San Diego, CA, USA). Sequencing was performed using a 2 × 250 paired-end (PE) configuration, and low-quality sequences were removed. Operational taxonomic units (OTUs) were clustered using a 97% similarity cut-off using UPARSE (version 7.1 http://drive5.com/uparse/), and chimeric sequences were identified and removed using UCHIME. Taxonomic assignments for each 16S rRNA gene sequence were determined using the RDP Classifier algorithm (http://rdp.cme.msu.edu/) against the Silva (SSU123) 16S rRNA database using a confidence threshold of 70%. DNA library building and data analysis were performed in accordance with the methods described by Zhang et al. [13]. The sequence data in this study have been deposited in NCBI under the SRA accession number SRP227025.

2.5. Data analysis

Effluent NO_3^-–N, NO_2^-–N, and NO_3^-–N removal efficiencies and the microbial community composition for different influent nitrate loading rates were evaluated via one-way ANOVA using SPSS 22.0. $P < 0.05$ was considered statistically significant. All significant points were imported into Cytoscape for network analysis. The *R*-package "pheatmap" was used to create heat maps of microbial communities. Other data analyses were performed using ORIGIN 8.0.

3. Results and discussion

3.1. Performance characteristics of the denitrification system

The denitrification performance for the influent NO_3^-–N loading rate (NLR) ranged from 0.30 to 1.28 g/(L d) depending on the influent NO_3^-–N concentrations and HRTs in the PHBV-supported system, as shown in Fig. 1a. The initial operating conditions for the PHBV reactor were a NO_3^-–N concentration of 80 mg/L and an HRT of 6.5 h. With the propagation of microorganisms and biofilm formation on the PHBV surface, the NO_3^-–N concentration decreased gradually, and the effluent NO_3^-–N concentration became stable. NO_3^-–N was completely removed on day 13. This finding indicated that the PHBV had a shorter domestication time than that of the biopolymer PCL [5] and a longer time than that of blended materials for biodegradable production, such as starch/polycaprolactone [14]. NO_2^-–N is the primary intermediate in the denitrification process. NO_2^-–N showed substantial accumulation (1.43 mg/L)
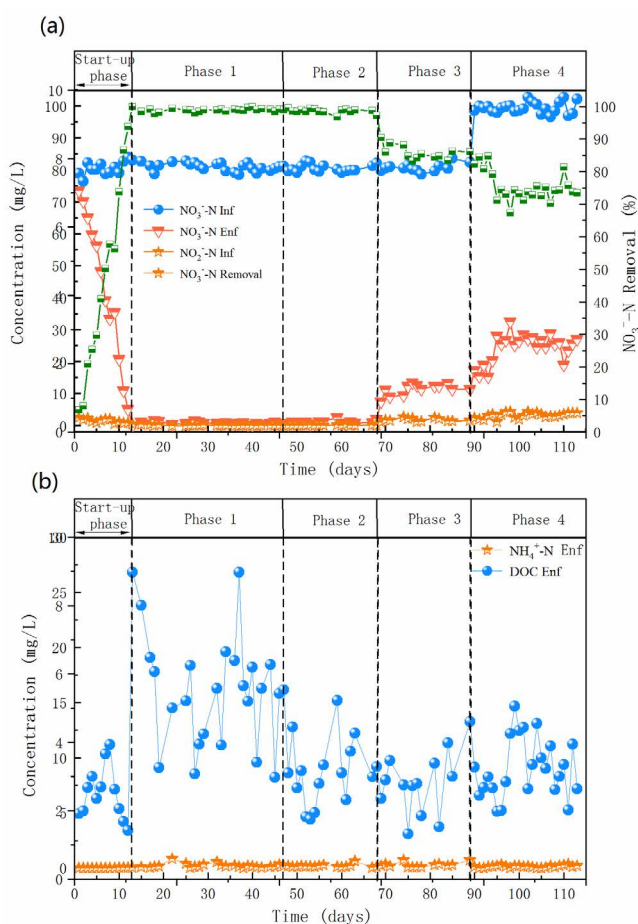
Fig. 1. Changes in effluent NO_3^-–N, NO_2^-–N, and NO_3^-–N removal efficiency (a) and NH_4^+–N and DOC (b) in the PHBV reactor during different phases.

during the lag period (Fig. 1b). During the stable operation stage (phase 1), the NO_3^-–N concentration decreased to 0.87 mg/L on days 14–47. Furthermore, the NO_2^-–N concentration was negligible. During phase 2, the HRT decreased to 2.5 h, and the NLR increased to 0.77 g/(L d). The effluent NO_3^-–N concentration did not fluctuate significantly. The average NO_3^-–N concentrations did not exceed 1.20 mg/L, and the NO_3^-–N removal efficiency was 98.63%. In addition, the effluent NO_2^-–N remained lower than 0.10 mg/L. During phases 1 and 2, the denitrification rate was equal to the NLR. During phase 3, the HRT was further shortened to 1.5 h, and the NO_3^-–N concentration increased within a narrow range. The average effluent NO_3^-–N concentration was 11.42 mg/L, and the NO_3^-–N removal efficiency decreased to 85.86%. Although the NO_3^-–N removal efficiency decreased, the denitrification rate increased to 1.11 g/(L d). This finding implies that the PHBV-supported denitrification system could exhibit excellent performance with a low HRT. However, during phase 4, the HRT was lengthened to 1.9 h, and the influent NO_3^-–N concentration increased to 100.0 mg/L; thus, the NLR remained the same as that in phase 3. The NO_3^-–N concentration increased substantially to 24.47 mg/L. The NO_3^-–N removal efficiency was 75.39%. In addition, the denitrification rate decreased to 0.95 g/(L d).

Clearly, the increased influent NO_3^-–N concentration led to an increasing effluent NO_3^-–N concentration and a decreasing nitrate removal efficiency. With the decreasing NO_3^-–N removal efficiency, the effluent NO_2^-–N clearly increased (phases 3 and 4). In comparison with the HRT, a high influent NO_3^-–N concentration negatively affected the nitrate removal performance when using PHBV-supported denitrification systems, exceeding the denitrification capability of the system. Microorganisms have a certain carrying capacity for environmental pollution. Once the threshold is exceeded, the processing capacity of microorganisms would be reduced, as described by Xu et al. [15].

The effluent ammonia concentrations in different phases are shown in Fig. 1b. Ammonia was not detected during the lag period. The ammonia concentration then increased slightly during the stable stage of phase 1. The average ammonia concentration was 0.21 mg/L. From phase 2 to phase 4, the ammonia concentration did not change substantially, with averages of 0.18, 0.28, and 0.14 mg/L for phases 2, 3, and 4, respectively. In general, in the heterotrophic denitrification system, ammonia is generated by the following mechanisms: dissimilatory nitrate reduction to ammonium [16]; an increased biofilm thickness creating a suitable environment for the bacteria with fermentative abilities, thereby reducing nitrate to ammonium [17]; and cell lysis into the effluent [18]. Therefore, backwashing at a certain time is an effective way to avoid ammonium accumulation.

The effluent DOC concentrations over the entire operation period are shown in Fig. 1b. During the start-up stage, the DOC concentrations ranged from 3.41 to 11.19 mg/L. The production of organic matter is primarily derived from the degradation of solid carbon sources, and its consumption is primarily used for the growth and denitrification of microorganisms. During this phase, microorganisms did not colonize the system. Therefore, the DOC concentration remained at a low level, which was not conducive to denitrification. The effluent DOC increased to 26.84 mg/L on day 13, indicating that the microbes began to degrade the PHBV rapidly. The high level of DOC lasted for several days and then decreased gradually. During phases 2 to 4, the effluent DOC concentrations averaged 8.68, 7.75, and 9.05 mg/L for each phase. These results indicated that organic carbon from PHBV degradation exceeds the amount of carbon required for microbial growth and denitrification. In a steady-state corncob and PHBV/PLA-supported denitrification system, the effluent DOC concentration is much higher than that in this study [19,20]. Some studies have shown that decreasing the HRT would decrease the production of soluble organic substances [9]. However, this was not observed in our study. It is possible that the decreased HRT did not lead to a decrease in the denitrification efficiency, and organic carbon was utilized efficiently by the microbes.

3.2. Microbial community analysis

Biofilm samples A, B, C, and D were collected from the PHBV SPD reactor on days 30, 61, 81, and 105, respectively. Low-quality reads were eliminated, and 53,151 ± 3,019 to 57,556 ± 4,055 effective reads were collected from four stages of biofilm samples. Based on the mothur algorithm, OTUs with a 97% shared similarity threshold were obtained.

The alpha diversity indexes Chao1 and ACE were used to evaluate the richness of the microbial community. As shown in Table 2, as the influent nitrate loading increased, microbial richness increased. This relationship was also supported by the rarefaction curve (Fig. S2). In addition, the sparse curve showed that the sequencing depth was sufficient to describe the characteristics of the microbial community. Based on the Shannon index, microbial diversity increased as the NLR increased (Table S3). Therefore, the NLR might affect the community structure and composition.

The microbial communities of biofilms on the surface of the PHBV were analyzed by Illumina high-throughput sequencing. *Proteobacteria* was the most abundant phylum during the entire phase, as shown in Fig. 2a. *Proteobacteria* accounted for more than 80% of the total sequence reads for each sample. The dominance of *Proteobacteria* in the PHBV denitrification system was consistent with previous results obtained by Zhang et al. [13] and Xu et al. [19]. Furthermore, *Proteobacteria* is the dominant phylum in PBS, PCL, SPCL-supported SPD systems [21–23]. *Proteobacteria* has been identified as the dominant phylum contributing to denitrification under various water conditions [24]. Microbial succession analyses showed that the HRTs had no significant effect on the relative abundance of the dominant phylum. As shown in Fig. 2b, with respect to bacterial classes, *Betaproteobacteria* (73.12%, 79.84%, 63.06%, and 62.71%) was predominant, followed by *Gammaproteobacteria* (5.91%, 8.18%, 23.23%, and 8.05%) and *Alphaproteobacteria* (9.09%, 2.79%, 4.54% and 1.76%) in samples obtained at different phases of denitrification. These dominant bacteria belonged to the phylum *Proteobacteria*. Previous studies have reported that *Betaproteobacteria*, a subclass of *Proteobacteria*, is advantageous in denitrification systems employing polymers as the carbon source [23,25]. In addition, the abundances of *Clostridia* (9.06%) and *Epsilonproteobacteria* (10.39%) increased during phase 4, suggesting that these classes contribute under high influent nitrate loading in the denitrification system. This conclusion is supported by that of Chen et al. [26].

Fig. 2c shows the relative abundances in the PHBV reactor at the genus level. At this level, *Diaphorobacter* and *Dechloromonas* were predominant during all phases, accounting for 51.76%, 46.20%, 21.58%, and 16.20% and 4.38%, 13.51%, 20.59%, and 21.66% of the genera, respectively. *Stenotrophomonas*, *Sulfurospirillum*, *Thauera*, and *Zoogloea* improved to various extents during phases 3 and 4. *Diaphorobacter* and *Dechloromonas* have been commonly identified as the dominant genera in SPD systems [23,25,27–31]. However, abundances differ among different SPD systems. In general, the abundance of *Dechloromonas* is highest [12]. *Dechloromonas* belongs to the class *Betaproteobacteria* and can oxidize benzene, ibuprofen, and other mono-aromatic compounds into CO_2 in an anoxic environment with nitrate as the electron acceptor [11,12,32]. *Diaphorobacter* is a denitrifying bacterium. Both nitrate and nitrite reductase activities were detected for eight isolated strains of *Diaphorobacter*. However, the nitrate reduction rate is 1.5 times greater than the nitrite reduction rate in *Diaphorobacter* sp. [33]. In this study, the relative abundance of *Diaphorobacter* decreased significantly from 51.76% to 16.20%, and the *Dechloromonas* abundance increased from
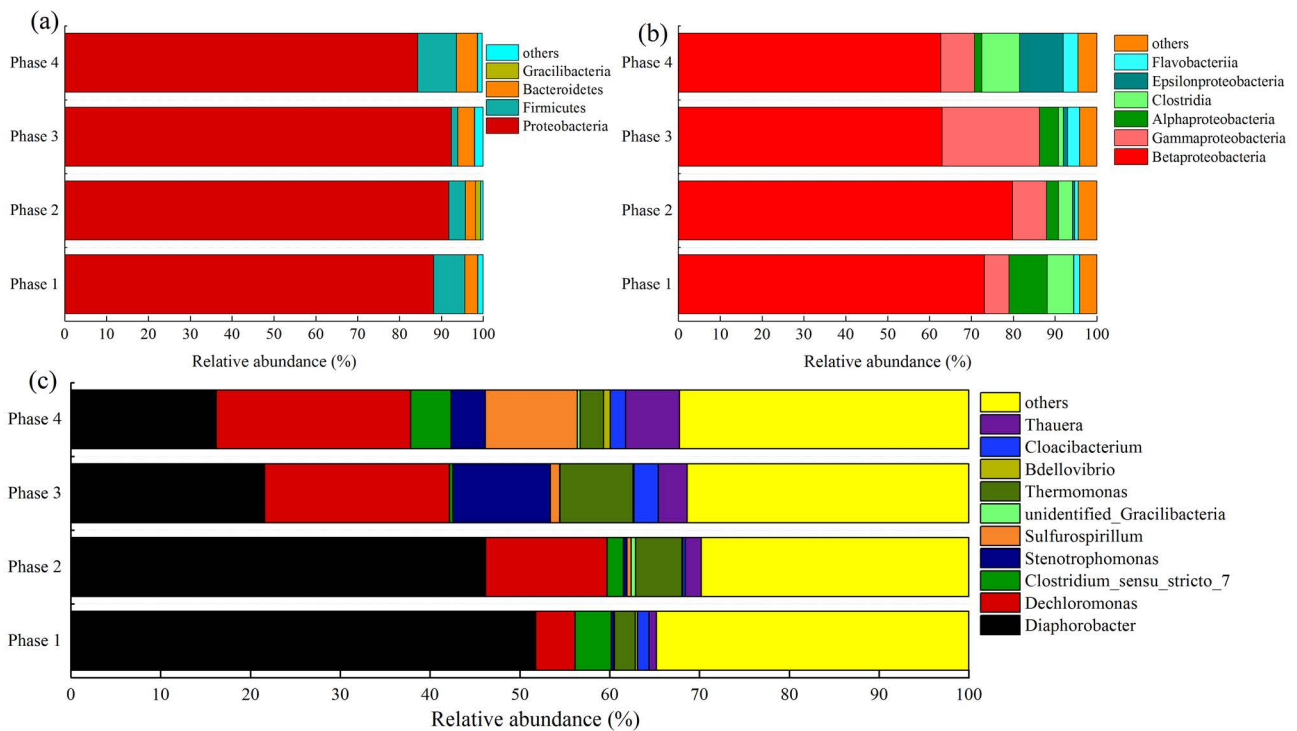
Fig. 2. Relative abundance at the primary phylum (a), class (b), and genus (c) levels in biofilm samples at different running phases. The data are shown as the means ± SD of 3 replicates.

4.38% to 21.66% owing to the increased influent nitrate loading ($P < 0.05$). These results indicated that the operational state of the reactor affected the species diversity. *Dechloromonas* accumulated under high influent nitrate loading, whereas *Diaphorobacter* was largely noted under low influent nitrate loading.

3.3. Network analysis of microbial communities and denitrification performance

To identify the effect of microbial interactions on effluent quality, a network diagram was generated to evaluate relationships among bacterial taxa. A bacterial relative abundance of greater than 0.5% was applied. Pearson correlation coefficients between the dominant bacterial genes and the effluent composition and NO_3^-–N removal efficiency were calculated using a one-tailed test. Correlations with *P*-values of less than 0.05 were included in the network shown in Fig. 3.

The nitrate removal efficiency exhibited a positive correlation with the abundances of *Dechloromonas* and *Sulfurospirillum*. Interestingly, these genera displayed negative correlations with the accumulated NO_2^-–N concentration, suggesting that increasing the abundance of *Dechloromonas* and *Sulfurospirillum* in the PHBV system could increase the denitrification efficiency. Furthermore, there was a negative correlation between NLR and *Diaphorobacter*. This may explain why the NO_3^-–N removal rate and denitrification efficiency decreased during phases 3 and 4. Based on the network diagram and the denitrification results summarized in Fig. 1, we found that there

was a negative correlation between the NLR and the nitrate removal rate. Some microorganisms do not show a direct link to nitrate removal but may still play an important role in the solid-phase nitrification process.

3.4. Analysis of microbial functions

To analyze the functions of the primary microorganisms in the system, 25 horizontal genus functions with the highest contents were selected. A heat map analysis of the 25 genus functions was performed using the "pheatmap" package in R, and the functional differences among samples were compared (Fig. 4). It is apparent that the denitrification function dominated over all stages, especially in phases 1 and 2. The results for the denitrification rate shown in Fig. 1 support this conclusion. At the genus level
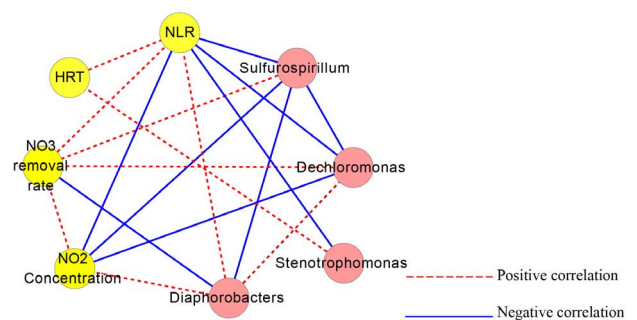
Fig. 3. Network correlations between the microbial community structure at the genus level and the denitrification performance.
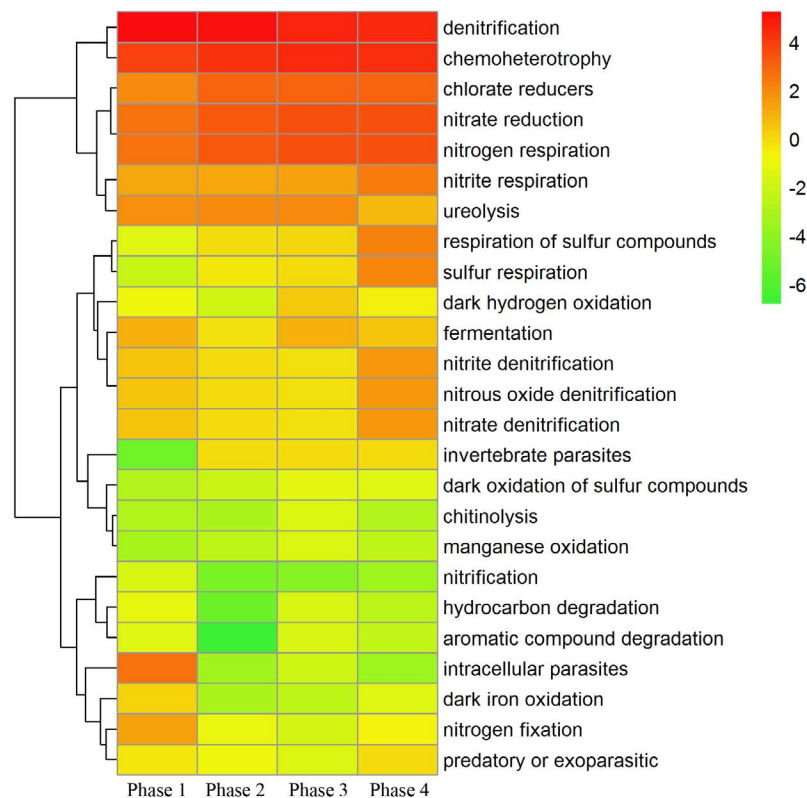
Fig. 4. Hierarchically clustered heat map of the function at the genus levels, at different stages.

(Fig. 2c), *Diaphorobacter* and *Dechloromonas* were the dominant bacteria involved in denitrification. During phases 3 and 4, the abundances of these genera decreased, which may account for the decrease in the denitrification rate and the high nitrate concentration in the effluent during these two periods. Previous studies have reported that PHBV is not directly utilized by microorganisms and must be hydrolyzed into soluble monomers, dimers, or trimers, which could act as carbon sources for bacterial growth and denitrification [8]. Therefore, chemoheterotrophy dominated each sample. It is worth noting that there were no harmful microorganisms over all phases of operation.

4. Conclusions

High denitrification rates in a PHBV-supported solid-phase denitrification reactor were achieved for high nitrate-concentration wastewater treatment. Moreover, compared to the HRT, the influent NO_3^-–N concentration has a greater effect on the denitrification efficiency at the same NLR. In an analysis of the microbial community structure of the biofilm, *Diaphorobacter* and *Dechloromonas* were predominant during all stages. Additionally, the nitrate removal efficiency exhibited a positive correlation with the abundance of *Dechloromonas*, and there was a negative correlation between the NLR and the *Diaphorobacter*. Comprehensive evaluations of relationships between the dominant genera and nitrate removal capacity will help reveal the mechanism underlying the efficient operation of PHBV-supported denitrification systems.

References

[1] S.-M. Zhu, Y.-L. Deng, Y.-J. Ruan, X.-S. Guo, M.-M. Shi, J.-Z. Shen, Biological denitrification using poly(butylene succinate) as carbon source and biofilm carrier for recirculating aquaculture system effluent treatment, Bioresour. Technol., 192 (2015) 603–610.
[2] J. Li, R.F. Jin, G.F. Liu, T. Tian, J. Wang, J.T. Zhou, Simultaneous removal of chromate and nitrate in a packed-bed bioreactor using biodegradable meal box as carbon source and biofilm carriers, Bioresour. Technol., 207 (2016) 308–314.
[3] Z.Q. Shen, Y.N. Yin, J.L. Wang, Biological denitrification using poly(butanediol succinate) as electron donor, Appl. Microbiol. Biotechnol., 100 (2016) 6047–6053.
[4] S.S. Zhang, X.B. Sun, Y.T. Fan, T.L. Qiu, M. Gao, X.M. Wang, Heterotrophic nitrification and aerobic denitrification by *Diaphorobacter polyhydroxybutyrativorans* SL-205 using poly (3-hydroxybutyrate-co-3-hydroxyvalerate) as the sole carbon source, Bioresour. Technol., 241 (2017) 500–507.
[5] A. Boley, W.R. Müller, G. Haider, Biodegradable polymers as solid substrate and biofilm carrier for denitrification in recirculated aquaculture systems, Aquacult. Eng., 22 (2000) 75–85.
[6] A. Hiraishi, S.T. Khan, Application of polyhydroxyalkanoates for denitrification in water and wastewater treatment, Appl. Microbiol. Biotechnol., 61 (2003) 103–109.
[7] S.T. Khan, A. Hiraishi, Isolation and characterization of a new poly(3-hydroxybutyrate)-degrading, denitrifying bacterium from activated sludge, FEMS Microbiol. Lett., 25 (2001) 253–257.

[8] J.L. Wang, L.B. Chu, Biological nitrate removal from water and wastewater by solid-phase denitrification process, Biotechnol. Adv., 34 (2016) 1103–1112.

[9] Z.S. Xu, X.H. Dai, X.L. Chai, Effect of influent pH on biological denitrification using biodegradable PHBV/PLA blends as electron donor, Biochem. Eng. J., 131 (2018) 24–30.

[10] C.-F. Chu, Y. Ebie, K.-Q. Xu, Y.-Y. Li, Y.H. Inamori, Characterization of microbial community in the two-stage process for hydrogen and methane production from food waste, Int. J. Hydrogen Energy, 35 (2012) 8253–8261.

[11] J.D. Coates, R. Chakraborty, J.G. Lack, S.M. O'Connor, K.A. Cole, K.S. Bender, L.A. Achenbach, Anaerobic benzene oxidation coupled to nitrate reduction in pure culture by two strains of *Dechloromonas*, Nature, 411 (2001) 1039–1043.

[12] P. Li, J.E. Zuo, Y.J. Wang, J. Zhao, L. Tang, Z.X. Li, Tertiary nitrogen removal for municipal wastewater using a solid-phase denitrifying biofilter with polycaprolactone as the carbon source and filtration medium, Water Res., 93 (2016) 74–83.

[13] S.S. Zhang, X.B. Sun, X.M. Wang, T.L. Qiu, M. Gao, Y.M. Sun, S.T. Cheng, Q.J. Zhang, Bioaugmentation with *Diaphorobacter polyhydroxybutyrativorans* to enhance nitrate removal in a poly (3-hydroxybutyrate-*co*-3-hydroxyvalerate)-supported denitrification reactor, Bioresour. Technol., 263 (2018) 499–507.

[14] Z.Q. Shen, J.L. Wang, Biological denitrification using cross-linked starch/PCL blends as solid carbon source and biofilm carrier, Bioresour. Technol., 102 (2011) 8835–8838.

[15] Z.S. Xu, L.Y. Song, X.H. Dai, X.L. Chai, PHBV polymer supported denitrification system efficiently treated high nitrate concentration wastewater: denitrification performance, microbial community structure evolution and key denitrifying bacteria, Chemosphere, 197 (2018) 96–104.

[16] J. van Rijn, Y. Tal, H.J. Schreier, Denitrification in recirculating systems: theory and applications, Aquacult. Eng., 34 (2006) 364–376.

[17] J.W. Nijburg, H.J. Laanbroek, The influence of *Glyceria maxima* and nitrate input on the composition and nitrate metabolism of the dissimilatory nitrate-reducing bacterial community, FEMS Microbiol. Ecol., 22 (1997) 57–63.

[18] L.B. Chu, J.L. Wang, Comparison of polyurethane foam and biodegradable polymer as carriers in moving bed biofilm reactor for treating wastewater with a low C/N ratio, Chemosphere, 83 (2011) 63–68.

[19] Z.S. Xu, X.H. Dai, X.L. Chai, Effect of different carbon sources on denitrification performance, microbial community structure and denitrification genes, Sci. Total Environ., 634 (2018) 195–204.

[20] X. Cao, Y.X. Li, X.Y. Jiang, P.G. Zhou, J.B. Zhang, Z. Zheng, Treatment of artificial secondary effluent for effective nitrogen removal using a combination of corncob carbon source and bamboo charcoal filter, Int. Biodeterior. Biodegrad., 115 (2016) 164–170.

[21] W.Z. Wu, L.H. Yang, J.L. Wang, Denitrification using PBS as carbon source and biofilm support in a packed-bed bioreactor, Environ. Sci. Pollut. Res., 20 (2013) 333–339.

[22] L.B. Chu, J.L. Wang, Denitrification performance and biofilm characteristics using biodegradable polymers PCL as carriers and carbon source, Chemosphere, 91 (2013) 1310–1316.

[23] Z.Q. Shen, Y.X. Zhou, J. Hu, J.L. Wang, Denitrification performance and microbial diversity in a packed-bed bioreactor using biodegradable polymer as carbon source and biofilm support, J. Hazard. Mater., 250 (2013) 431–438.

[24] D. Chen, H.S. Wang, K.J. Yang, F. Ma, Performance and microbial communities in a combined bioelectrochemical and sulfur autotrophic denitrification system at low temperature, Chemosphere, 193 (2018) 337–342.

[25] Y.L. Li, J.S. Zhang, G.B. Zhu, Y. Liu, B. Wu, W.J. Ng, A. Appan, S.K. Tan, Phytoextraction, phytotransformation and rhizodegradation of ibuprofen associated with Typha angustifolia in a horizontal subsurface flow constructed wetland, Water Res., 102 (2016) 294–304.

[26] D. Chen, D. Wang, Z.X. Xiao, H.Y. Wang, K. Yang, Nitrate removal in a combined bioelectrochemical and sulfur autotrophic denitrification system under high nitrate concentration: effects of pH, Bioprocess. Biosyst. Eng., 41 (2018) 449–455.

[27] T.L. Qiu, Y. Xu, M. Gao, M.L. Han, X.M. Wang, Bacterial community dynamics in a biodenitrification reactor packed with polylactic acid/poly (3-hydroxybutyrate-*co*-3-hydroxyvalerate) blend as the carbon source and biofilm carrier, J. Biosci. Bioeng., 123 (2017) 606–612.

[28] F. Han, W. Ye, D. Wei, W.Y. Xu, B. Du, Q. Wei, Simultaneous nitrification-denitrification and membrane fouling alleviation in a submerged biofilm membrane bioreactor with coupling of sponge and biodegradable PBS carrier, Bioresour. Technol., 270 (2018) 156–165.

[29] H.M. Sun, T. Wang, Z.C. Yang, C. Yu, W.Z. Wu, Simultaneous removal of nitrogen and pharmaceutical and personal care products from the effluent of waste water treatment plants using aerated solid-phase denitrification system, Bioresour. Technol., 287 (2019) 121389, https://doi.org/10.1016/j.biortech.2019.121389.

[30] J. Xu, H.L. Pang, J.G. He, J. Nan, M.F. Wang, L. Li, Start-up of aerobic granular biofilm at low temperature: performance and microbial community dynamics, Sci. Total Environ., 698 (2020) 134311, https://doi.org/10.1016/j.scitotenv.2019.134311.

[31] Z.S. Xu, X.H. Dai, X.L. Chai, Biological denitrification using PHBV polymer as solid carbon source and biofilm carrier, Biochem. Eng. J., 146 (2019) 186–193.

[32] S.Y. He, Y.M. Wang, C.S. Li, Y.C. Li, J. Zhou, The nitrogen removal performance and microbial communities in a two-stage deep sequencing constructed wetland for advanced treatment of secondary effluent, Bioresour. Technol., 248 (2018) 82–88.

[33] S.S. Chakravarthy, S. Pande, A. Kapoor, A.S. Nerurkar, Comparison of denitrification between *Paracoccus* sp. and *Diaphorobacter* sp, Appl. Biochem. Biotechnol., 165 (2011) 260–269.

Supplementary information
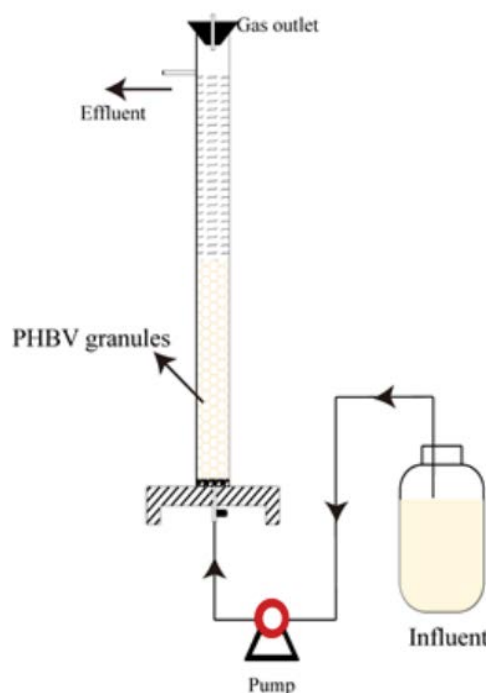
Fig. S1. Schematic diagrams of the PHBV-supported solid-phase denitrification reactor.
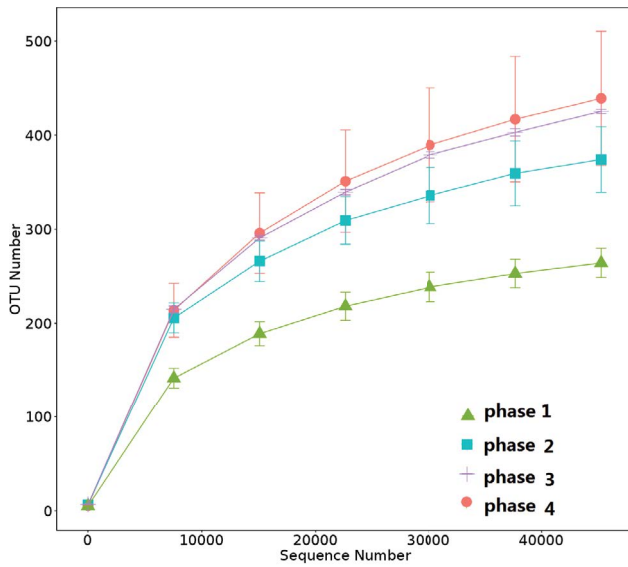
Fig. S2. Rarefaction curves of OTUs clustered at 97% sequence identity across different samples.

Table S1
PCR reaction system

Item	Volume (μL)
PCR mix	10
Primer 338F	0.5
Primer 806R	0.5
Template DNA	1
Add sterile water	Total to 20

Table S2
PCR procedure

Program	Temperature (°C)	Time	Cycles
Predenaturation	95	3 min	–
Denaturation	95	30 s	
Anneale	55	30 s	27
Elongation	72	45 s	
Extension	72	10 min	–

Table S3
Richness and diversity estimators of the bacterial phylotypes for biofilm samples based on Illumina high-throughput analysis

Phase	Reads	OTUs	Shannon	Chao1	ACE	Coverage
1	53,151 ± 3,019	574 ± 29	3.27 ± 0.48	758.27 ± 53.72	658.76 ± 22.38	99.67% ± 0.09%
2	54,939 ± 1,182	304 ± 23	3.37 ± 0.24	405.63 ± 45.95	340.80 ± 16.52	99.82% ± 0.00%
3	57,556 ± 4,055	442 ± 56	4.23 ± 0.21	503.48 ± 58.45	473.30 ± 63.72	99.76% ± 0.04%
4	56,303 ± 2,163	515 ± 8	4.29 ± 0.01	651.41 ± 3.95	581.97 ± 19.38	99.68% ± 0.00%